

CLIPPER: a long-range, autonomous underwater vehicle using magnesium fuel and oxygen from the sea

Øistein Hasvold^{a,*}, Torleif Lian^a, Erik Haakaas^a, Nils Størkersen^a,
Olivier Perelman^b, Stephane Cordier^b

^a FFI (Norwegian Defence Research Establishment), P.O. Box 25, N-2027 Kjeller, Norway

^b Direction General d'Armement/Bassin d'essais des carènes (DGA/BEC), Chaussée du Vexin, Val de Reuil 27100, France

Available online 8 June 2004

Abstract

The development of the CLIPPER autonomous underwater vehicle (AUV) is a joint research project (JRP) between DGA/BEC in France and FFI in Norway. The power source is a semi-fuel cell using oxygen dissolved in seawater as oxidant, seawater as electrolyte and magnesium as fuel. Predicted range for the vehicle is in excess of 1600 nautical miles at a speed of 2 m/s. Design depth is 600 m. This long endurance, as well as the large internal volume of 7401 of the pressure hull, makes the CLIPPER vehicle an excellent tool for long range subsea operations.

© 2004 Elsevier B.V. All rights reserved.

Keywords: Magnesium anode; Oxygen cathode; Seawater electrolyte semi-fuel cells; Magnesium seawater batteries

1. Introduction

The first autonomous underwater vehicle (AUV) developed by FFI was a technology demonstrator made to show that the magnesium/dissolved oxygen semi fuel cell [1] could be used as a power source for AUVs. This was successfully demonstrated in May 1993, but these experiments also highlighted the low specific power of this power source, making it inferior to other power sources unless long-term missions (>200 h) were a requirement. Thus later AUV developments from FFI (e.g. the HUGIN series) have been using other power sources such as the alkaline aluminium/hydrogen peroxide semi-fuel cell [2,3] and lithium ion batteries [4]. However, compared to the seawater battery, these chemistries have low specific energy.

The aim of the CLIPPER project was to establish a technology base for providing the capability of very long-range operation of AUVs by combining optimal hydrodynamic design and efficient propulsion with high energy density battery technology. The project is organised as a joint research project (JRP) between France and Norway. The partners are Direction Generale Armement (DGA), Bassin d'Essais des Carenés (BEC) and the Norwegian Defence Research Establishment (FFI). BEC provides expertise on hydrody-

amic optimisation and testing and propulsion technology, while FFIs contribution is within power sources and AUV technology. *Corps Laminaire Integrand une Propulsion a Pile Eau du mer* (CLIPPER). The target for the first phase of the CLIPPER project is to build a full-scale model vehicle and power source and verify the battery and propulsion performance in full-scale tests. One of the objectives of the JRP is that the model vehicle should be capable of being further developed to an ocean going prototype to demonstrate potential operational capabilities in a follow-on phase 2 of the CLIPPER collaboration. Thus the filament wound pressure hull in the model vehicle is designed for an operational depth of 600 m.

Prospective military applications of CLIPPER that exploit the extreme range capability or endurance are intelligence, surveillance, target acquisition, reconnaissance (ISTAR) operations, anti submarine warfare (ASW), offboard tactical element for submarine operations, and rapid environmental assessment (REA). Marine research, polar research and search and survey operation are among some civilian applications that may use a range capability in excess of 1600 nautical miles.

Because of the intimate connection between the vehicle drag and propulsion, the internal flow, the battery performance and the flow through the battery, the development has consisted of a series of loops. In each loop a vehicle was designed and power for propulsion and flow in the battery

* Corresponding author. Tel.: +47-63-80-75-34; fax: +47-63-80-75-09.
E-mail address: oistein.hasvold@ffi.no (Ø. Hasvold).

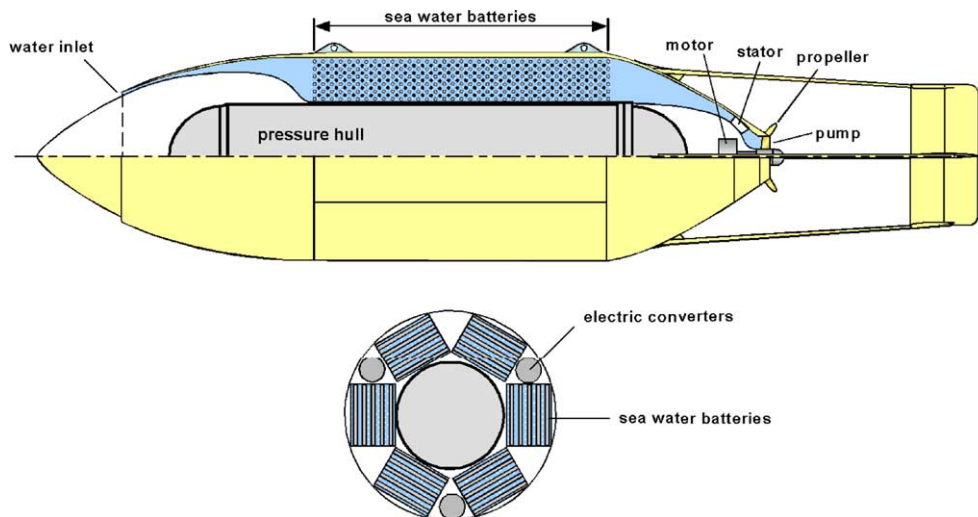


Fig. 1. Schematic drawing of the CLIPPER AUV. Displacement $\Delta = 3.9 \text{ m}^3$.

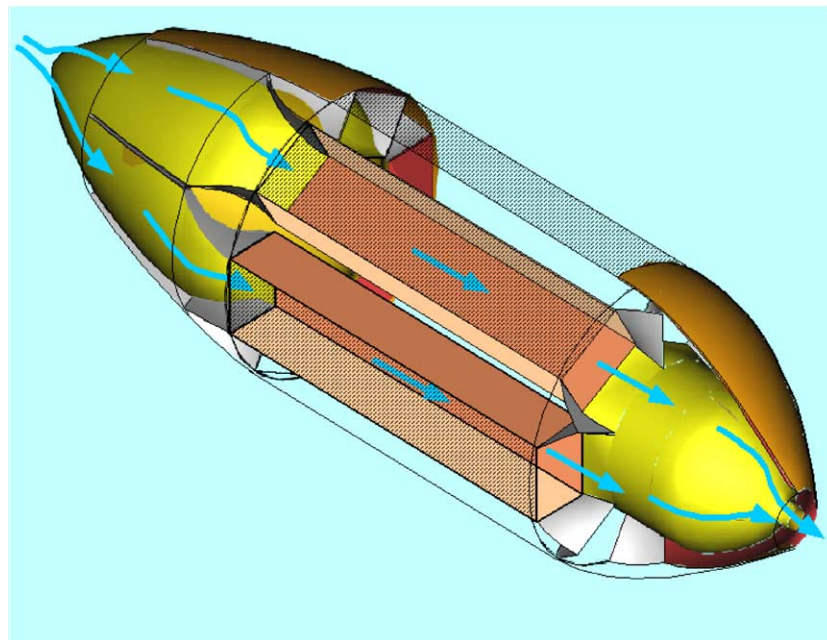


Fig. 2. Seawater flow through the CLIPPER AUV.

computed. A model battery was then produced and tested at the calculated flow velocity and specific load. Based on the test results, a new vehicle and battery design was developed. The final design is shown in Fig. 1. Fig. 2 shows the flow of water through the vehicle. Thrust for propulsion is generated partly from the water from the battery (water jet), partly from the propeller.

2. Principles of operation

The battery concept is based on the use of seawater as electrolyte and oxygen dissolved in the ocean as oxidant in a semi-fuel cell with magnesium anodes as fuel. The ad-

vantage of this concept is the increased ratio of energy to weight and volume compared to common battery technology. A further weight saving is caused by the operation at ambient pressure. Most other battery systems require a pressure resistant container for the battery.

During operation, a flow of seawater through the battery supplies the battery with oxygen and removes the products of the reactions taking place in the battery. Comprehensive descriptions of the cell chemistry are given in [1,5,6,7].

One challenge in the design of the battery was to be able to supply the battery with a sufficiently large flow of seawater and at the same time use as little energy for this process as possible. A second challenge is to handle large currents with small voltage loss. Because the cells are in a common

electrolyte (the ocean), serial connection of seawater cells to raise the battery voltage is not possible unless special precautions are taken to reduce leakage currents between cells. For this application, we decided to use only parallel-connected cells and a DC/DC converter to raise the voltage to a useful level. This concept was also used in the unmanned underwater vehicle AUV-Demo in 1993 [1].

The CLIPPER battery has the shape of six cells oriented around a central pressure hull as shown in Figs. 1 and 2. A secondary battery is located inside the pressure hull. Three dc to dc converters are located between the cells. They convert the nominal one volt from the seawater cell to nominal 48 V for the CLIPPER system voltage. Each converter is connected to two cells. The secondary battery is charged from the converters.

The seawater cell is prismatic and contains $6 \times 39 = 234$ parallel-connected magnesium rods and $5 \times 38 = 190$ parallel-connected carbon fiber brush cathodes with metal core. Cathode length was 350 mm and cathode diameter was 30 mm. Anode diameter was 22 mm at start of discharge. Fig. 3 shows a top view of the inlet of one cell. Seawater enters the cell in one end and leaves in the other. On its way through the cell, the concentration of oxygen is reduced and the concentration of the products of the cell reaction increased. These changes in the seawater chemistry increase with the length of the cell and decrease with increasing flow velocity. Thus the cell voltage should increase with increasing flow, as indeed observed, but as also the hydrodynamic work (i.e. product of flow and differential pressure over the cell) increases with increasing flow, there is an optimum flow through the cell where net power is at maximum. We also observed that there exists a minimum flow. Below that flow, the cell clogs with the reaction products. Most experiments were made in the seawater laboratory on shore [1] with cells with reduced electrode length (100 mm) and only two rows of cathodes and three rows of anodes. In these experiments parameters such as flow velocity, size of electrodes, distance cell to cell and numbers of electrodes in the flow direction were varied and cell performance and hydrodynamic power

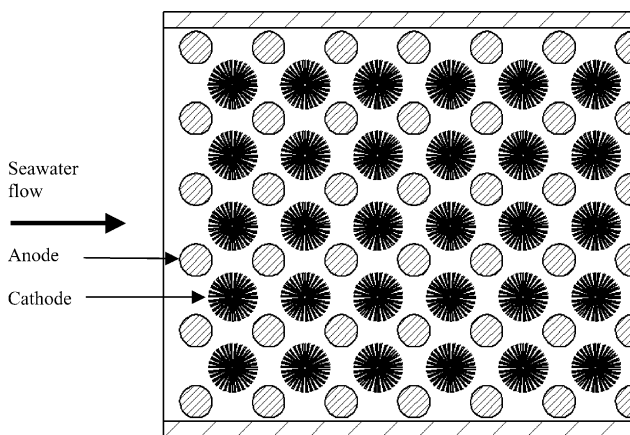


Fig. 3. Top view of the inlet of one cell. There are $6 \times 39 = 234$ anodes and $5 \times 38 = 190$ cathodes in each cell.

lost measured. In this paper, only the results on full-scale cells are reported.

3. Experimental

The test set-up consisted of the cell, a programmable load and measuring circuits for cell voltage, current, temperature, pressure loss and flow. Because the six cells are symmetrically arranged, we only needed to test one cell to verify the battery performance in the full-scale test. The test was performed in a stationary test facility southwest of Bergen, Norway.

Seawater was taken from the ocean into an axial pump, then through a flow straightener to reduce vortices, then through a venturi and into the cell. The aft end of the cell was open to the ocean. The flow was controlled by a brush-less electric motor in an oil-filled housing connected to an axial pump. Flow was measured using the differential pressure over the venturi. The differential pressure over the cell was also measured. Calibration was performed in a freshwater tank at FFI using ultrasonic flow measurement and water filled tubes for pressure measurement. One reference electrode (Ag/AgCl) was mounted in the compartment ahead of the cell and one in the cell outlet. Thus IR-loss in the electrolyte in the cell is mainly included in the cathode potential measurements.

The equipment was mounted in an aluminium framework and deployed at the seabed at a depth of 25 m. A cable was used for data transfer (RS485) and power (ac, 230 V) from shore. Advantech ADAM-modules were used for measurement and control together with home made electronics. The control programs were written using Advantech Genie version 3.0 and higher. This equipment allowed discharge at constant current or discharge at constant power.

Remote data-acquisition (using PC-Anywhere) made it possible to evaluate the experiment from FFI.

Logging and measuring equipment had a 110 Ah/12 V battery back-up, sufficient for 48 h in case of power failure. At the seabed, a lithium battery supplied local emergency power.

On each cell, the following experiments were always performed and in the following order:

- Pressure loss over the cell as function of flow (at open circuit);
- Load curve: Cell voltage versus cell current
- Cell discharge curve: cell voltage versus time at 133 W constant cell power.

Occasionally, the discharge was stopped and a new load curve or pressure loss curve recorded followed by continued discharge.

The anodes were individually weighted before and after each discharge.

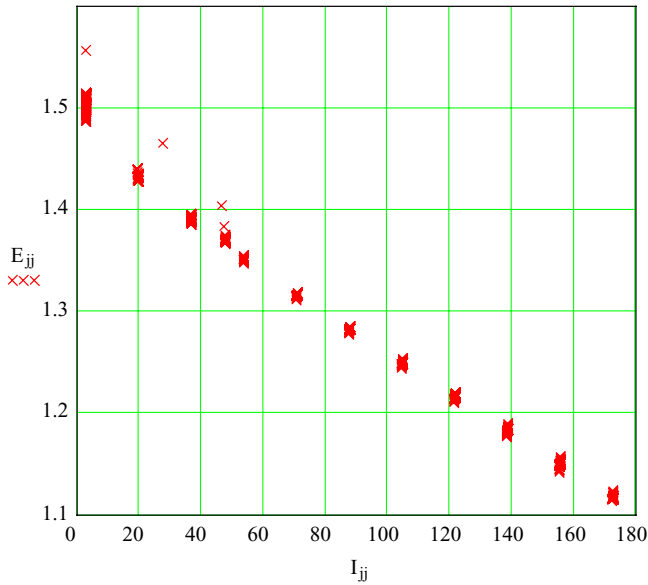


Fig. 4. Cell voltage E [V] vs. cell current I [A]. Fresh cell (start of discharge). Test 2.

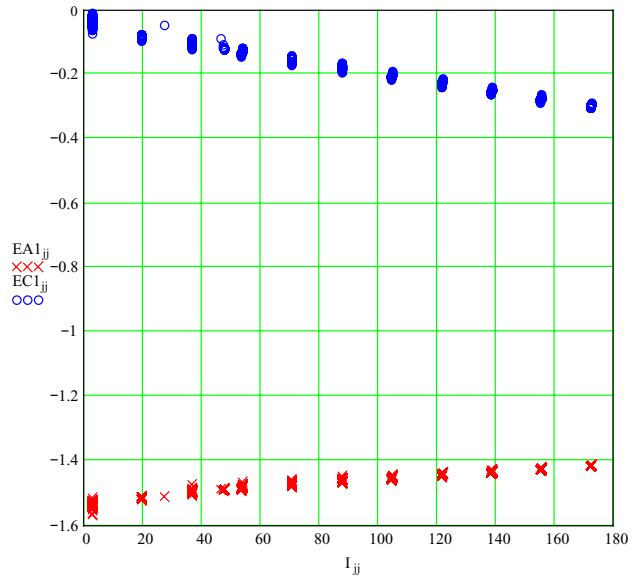


Fig. 5. Anode potential EA and cathode potential EC [V] vs. cell current I [A]. Fresh cell. Reference electrode located at the cell outlet. Test 2.

4. Results

Three full cell discharge experiments were undertaken. The first was basically an equipment break-in test, while test two and three were tests for battery characteristics. Fig. 4 shows the cell voltage and Fig. 5 the electrode potentials as function of the cell current. Flow was 8.5 l/s. Fig. 6 shows the pressure loss over the cell and Fig. 7 the hydrodynamic power lost in the cell as a function of flow. The pressure loss

is given as cm water column height. (One cm equals 100 Pa). In test 2, the cell delivered 133 W for 504 h (67,032 Wh). Charge delivered was 56,840 Ah.

Test 3 was similar to test 2 with two important differences:

- Initially, the cell was unintentionally exposed to an internal short for nearly one hour, it was then taken back to base, repaired and left at the quay for a week before redeployment.

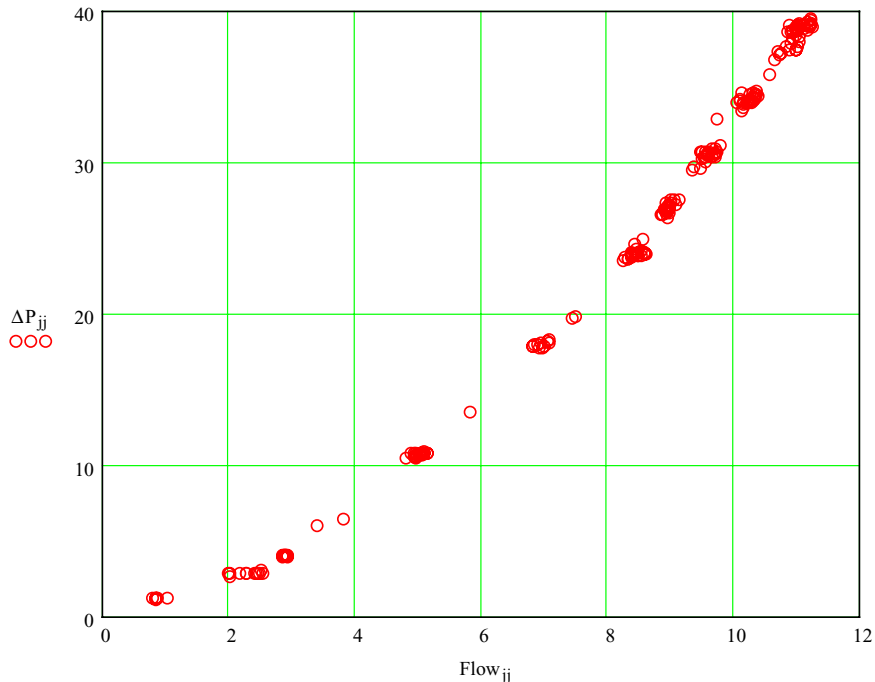


Fig. 6. Pressure loss ΔP [cm water] over the cell as function of flow [l/s]. Open circuit. Test 2.

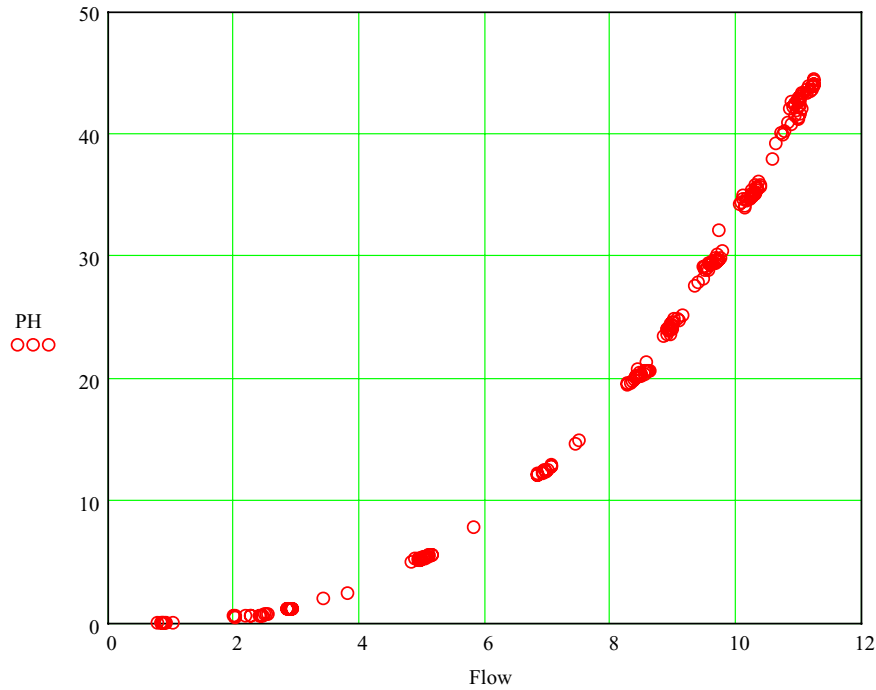


Fig. 7. Hydrodynamic power lost PH [W] in the cell as function of flow [l/s]. Open circuit. Test 2.

2. The flow was reduced from 8.5 to 7.5 l/s. The results from test 2 and test 3 were fairly similar, therefore only data from one of the tests are shown.

Fig. 8 shows the cell voltage and cell current versus time. The cell power was a constant 133 W, thus cell current increases as cell voltage decreases. The discharge was terminated when the cell voltage fell to 0.6 V. Fig. 9 shows the simultaneous pressure-loss over the cell, the corresponding hydrodynamic loss of power and the flow through the cell

during the test. The propeller rotation rate was constant during discharge, resulting in an increase in flow as the anodes were consumed and the gap between the electrodes increased. The oscillations shown on the curves show the tidal frequency and are probably caused by variation in the local water velocity (sea current). Fig. 10 shows the anode and the cathode potentials versus time. The two reference electrodes gave fairly similar readings, only during the last part of the discharge was a small shift observed, indicating lower current density in the aft part of the cell.

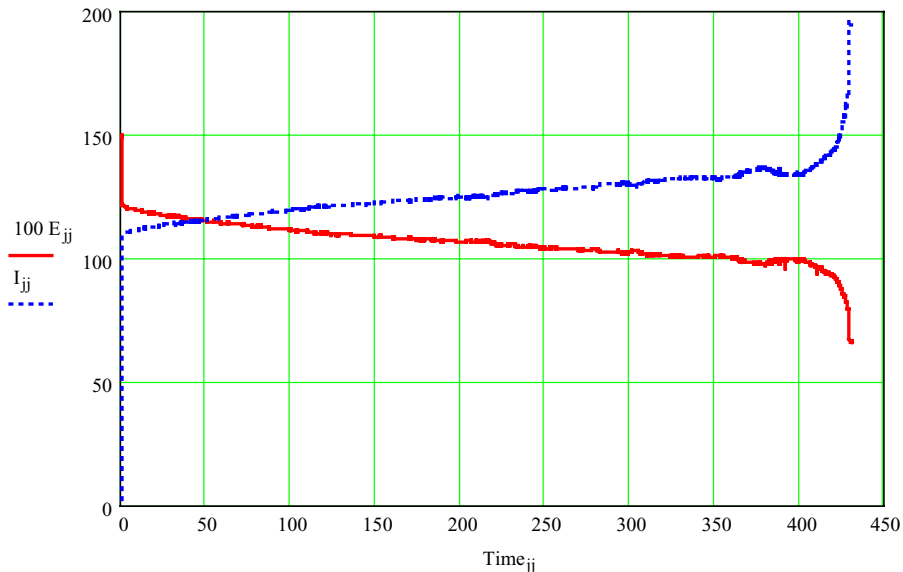


Fig. 8. 100 times the cell voltage E [V × 100] and cell current I [A] vs. time [h] at 133 W load. Test 3.

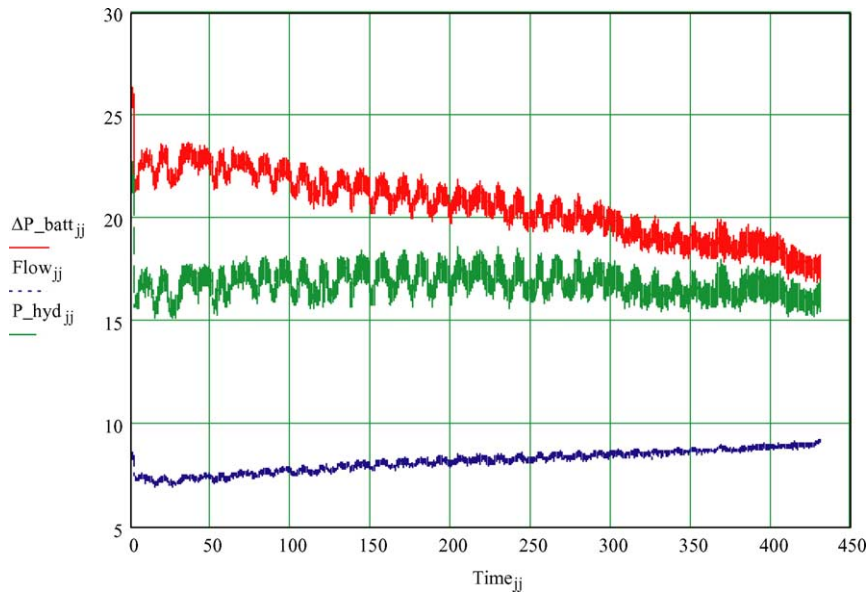


Fig. 9. Upper curve: Pressure loss in the cell ΔP_{batt} [cm water], middle curve: Hydrodynamic power loss P_{hyd} [W], lower curve: seawater flow [l/s] vs. time [h]. Test 3.

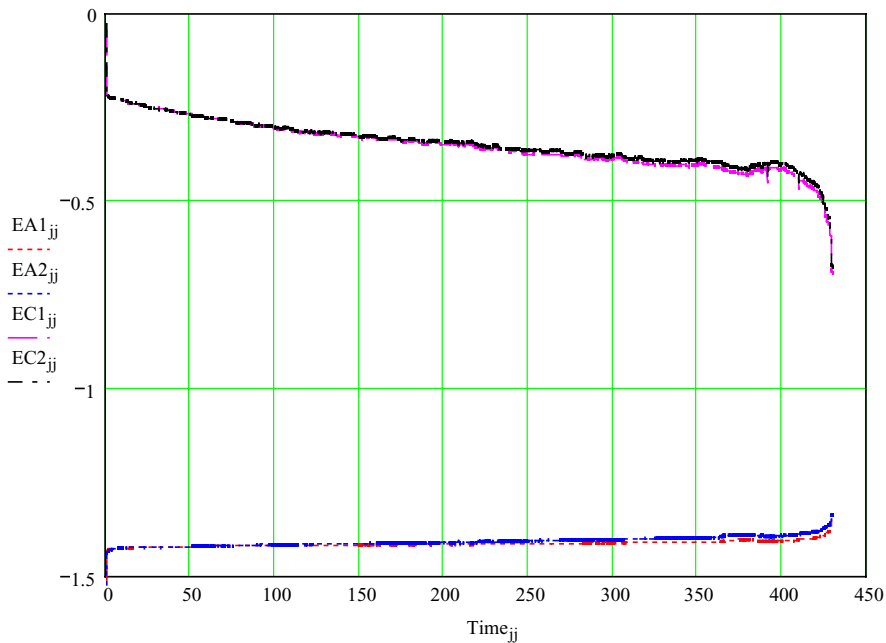


Fig. 10. Cathode potentials EC1 and EC2 and anode potentials EA1 and EA2 [V] vs. time [h]. Reference electrode no. 2 is close to the cell inlet, reference electrode no. 1 close to the cell outlet. Cell load is 133 W. Test 3.

In test 3, we achieved 429 h at 133 W (57,057 Wh). Charge delivered was 54,240 Ah.

In this test, initial anode weight was 56.2 kg. During discharge, 41.2 kg was consumed. Fig. 11 shows the relative anode consumption as a function of anode position. Anodes that were surrounded by 4 cathodes show the largest consumption, whereas anodes at the corners of the cell show the least. The figure shows a decrease in consumption toward the end of the cell in test 3. This correlates well with the po-

tential measurements. In test 2, the decreased consumption in the aft part of the cell was not observed.

5. Discussion

Based on former experiences, an efficiency of 85% can be assumed for the dc to dc converter. Similarly, motor efficiency is >90%. The result of the computational fluid

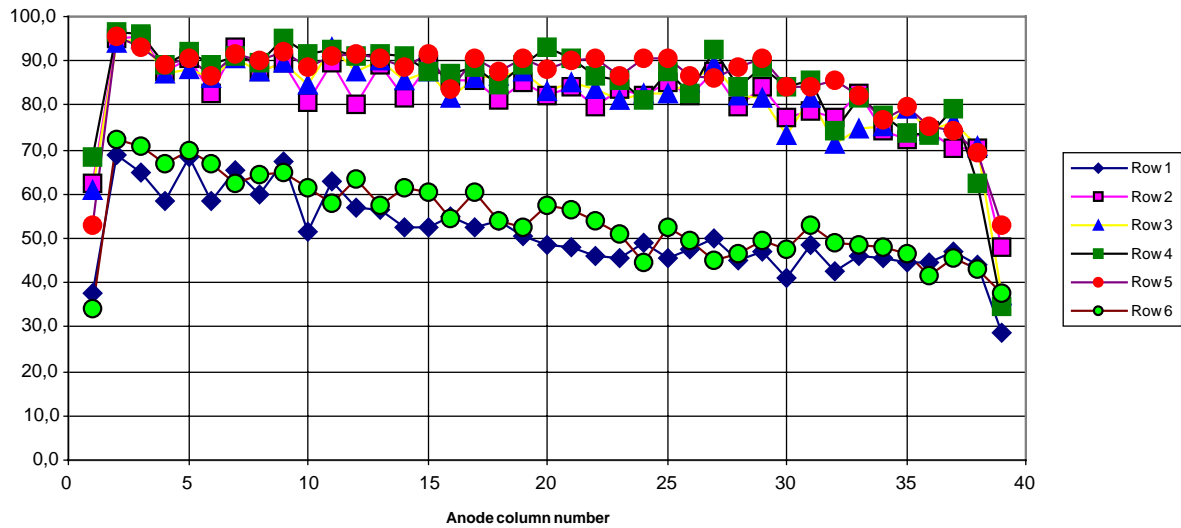


Fig. 11. Relative anode consumption in wt.% as function of anode position. Test 3.

dynamics (CFD) was an expected electric power consumption of 406 W for the propeller/pump combination given a vehicle speed of 2 m/s and a flow through the battery of 53 l/s (8.8 l/s per cell).

The CLIPPER battery is composed of six seawater cells. Thus electric power available for CLIPPER is $6 \times 133 \text{ W} \times 0.85 = 678 \text{ W}$. Given that propulsion and pumping of water through the battery requires 406 W, this leaves an average of 272 W for vehicle control and hotel loads. In addition, much higher power may be delivered for short periods as the CLIPPER AUV will have a 12 cell serially connected lithium ion battery of at least 120 Ah (ca 5.2 kWh). System energy based on experiment 3 is 291 kWh plus the energy stored in the buffer battery.

Our results show that the flow may be decreased to 45 l/s with only marginal effect on performance, thus increasing the allowable hotel load somewhat. This is important because pumping power is expensive (must be divided by pump efficiency and by converter efficiency).

Comparing seawater batteries and conventional batteries for AUV applications is difficult on a quantitative basis as the vehicles are very different. Seawater batteries operate outside the pressure hull whereas conventional batteries usually are inside. Thus vehicle depth rating enters the calculations. One way would be to use the total displacement, dry and wet volume for hotel load and hotel power consumption and compare neutrally buoyant vehicles with identical speed. Doing that, one finds that the energy of the seawater battery system is very high and comparable to what is possible with dense packing of primary lithium batteries in carbon fiber epoxy pressure containers of moderate depth rating. In contrast to primary lithium batteries however, the seawater battery does not increase the vulnerability of the mother vessel and it contains no toxic ingredients that may do harm, even in a case of a moderate fire.

The cost is also significantly lower. The negative side, besides the low power rating, is the fact that there are locations where seawater batteries cannot be used, as the oxygen concentration is too low. During one discharge of 400 h with a flow through the battery of 45 l/s, approximately 65 000 t of water goes through the vehicle. To avoid contamination of the cathodes, one should also avoid highly polluted areas or areas where the algae concentrations is high (low visibility water). These limitations on applicability can be removed if an acid solution of hydrogen peroxide is added to the electrolyte [8], but at the expense of energy density and system complexity.

6. Conclusion

It has been shown that it is possible to make a vehicle, using naturally occurring oxygen dissolved in seawater as oxidant and magnesium as fuel, which has the energy and power necessary to cross from Svalbard to North America via the North Pole or to patrol in an area for nearly 3 weeks.

At a nominal load of 133 W per cell, an endurance of 504 h has been achieved at a hydrodynamic loss of 24 W and 430 h a hydrodynamic loss of 17 W. This performance is sufficient for a vehicle speed of 2 m/s (ca. 4 knots) with a hotel load of approximately 270 W. These experimental results show that a range capability in excess of 1600 nautical miles is well within reach. This long range, as well as the large internal volume of 740 l of the pressure hull, makes the CLIPPER underwater vehicle a useful tool for civilian as well as military oceanographic research.

Compared to other power sources, the energy available for underwater vehicles using the seawater semi-fuel cell is a factor of 3 better than the best available rechargeable batteries and comparable to primary lithium batteries. In contrast to other high-energy power sources however, the

magnesium dissolved oxygen seawater cell is intrinsically safe.

References

- [1] Ø. Hasvold, A magnesium-seawater power source for autonomous underwater vehicles, in: A. Attewell, T. Keily (Eds.), *Power Sources*, vol. 14, 1993, pp. 243–255.
- [2] Ø. Hasvold, K.H. Johansen, O. Mollestad, N. Størkersen, The alkaline aluminium/hydrogen peroxide power source in the HUGIN II unmanned underwater vehicle, *J. Power Sources* 80 (1999) 254–260.
- [3] Ø. Hasvold, K.H. Johansen, K. Vestgaard, The Alkaline aluminium hydrogen peroxide semi-fuel cell for the Hugin 3000 autonomous underwater vehicle, in: *Proceedings of the 2002 Workshop on Autonomous Underwater Vehicles*, San Antonio, TX, 20–21 June 2002, pp. 89–94.
- [4] Ø. Hasvold, N. Størkersen, Electrochemical power sources for unmanned underwater vehicles used in deep sea survey operations, *J. Power Sources* 96 (2001) 252–258.
- [5] Hasvold, Øistein, Seawater batteries for long term applications, in: T. Keily, B.W. Baxter (Eds.), *Power Sources*, vol. 13, 1991, pp. 307–317.
- [6] Ø. Hasvold, H. Henriksen, B. Syversen, in: A. Attewell, T. Keily (Eds.), *Improvements in the rate capability of the magnesium-dissolved oxygen seawater cell*, *Power Sources*, vol. 15, 1995, pp. 149–162.
- [7] Ø. Hasvold, H. Henriksen, E. Melvær, G. Citi, B.Ø. Johansen, K. Kjøningsen, R. Galetti, *J. Power Sources* 65 (1997) 253–261.
- [8] M.G. Madeiros, R.R. Bessette, C.M. Deschenes, D.W. Atwater, Optimization of the magnesium-solution phase catholyte semi-fuel cell for long duration testing, *J. Power Sources* 96 (2001) 236–239.